Can Quantum Computers Overheat?
CMSC657: Final Report

Wade Hodson, Sandesh Kalantre, and Arthur Lin
(Dated: December 14, 2018)

We investigate the thermodynamics of realistic quantum circuits. Experimentally, any quantum computing platform is not fully isolated from an environment, and this unwanted coupling may give rise to errors in gate operations. A fidelity of exactly one would be expected for a perfect gate operation and such an operation would be perfectly reversible; but otherwise in experiments this is not achieved due to various technical limitations and decoherence from the environment. In this paper, we try to ask the inverse question – for an imperfect quantum operation with a given fidelity, what are the corresponding thermodynamic costs? We present a simplified model for imperfect quantum operations with the dephasing channel, and extract the relationship between entropy change and fidelities. We report numerical simulations for small quantum circuits (in terms of qubits). We also present a summary of experimentally measured fidelities for various quantum computing platforms, and delineate the thermodynamic implications of those under our model. We conclude with a discussion of why thermodynamic costs would be relevant for scaling up quantum systems in terms of architectures and required technical limitations.

CONTENTS

I. INTRODUCTION

In order to achieve practical, cost-effective computation, computer hardware designers must consider the thermodynamic costs associated with logical operations. In the realm of classical computing, thermodynamic analysis of classical models of computation has led to results such as the Landauer bound [1], which identifies a fundamental lower limit to the amount of heat which must be dissipated in a logically irreversible computation. Currently, typical computers release heat quantities which are orders of magnitude above this bound [2]. However, as technological advancements lead to continually smaller and more energy-efficient devices, theoretical results such as the Landauer limit may become increasingly relevant to the design and manufacture of computer hardware.

Thermodynamic analysis of computation may also be applied to quantum algorithms. In general, any classical or quantum system must be coupled to an external control mechanism for computations. The system also interacts with uncontrolled environmental degrees of freedom. Thus, every logical operation, when instantiated in a specific physical device, will entail certain energetic and entropic costs. Just as certain quantum algorithms perform better than their classical counterparts in terms of memory usage or time complexity [3], one may also ask whether a similar "quantum advantage" exists with respect to the energetic costs of quantum computations.

In this paper, we aim to investigate such costs in the context of quantum computation. Specifically, we will investigate the thermodynamic effects of imperfect gates, measurement, and initialization of qubits under a quantum circuit model. Using tools from the field of quantum thermodynamics [4–6], we will consider the thermodynamic heat dissipation associated with a given physical implementation of quantum algorithms. We will analyze how this heat cost scales as a function of input size, circuit complexity, output fidelity, and computation speed. We shall evaluate this cost for near-term quantum computing implementations, and estimate the limit at which this cost significantly impacts the feasibility of large-scale quantum computation.

II. PROBLEM DESCRIPTION

The central aim of this project is to establish a thermodynamic heat cost associated with a quantum circuit. Quantum gates, as is well known from experimental efforts [7, 8], are not perfect in their operation. In general, the desired final state of a gate cannot be obtained with unit fidelity. This error stems from noise sources, and can be traced back to the coupling of the qubit to its environment. We refer to such gate operations as imperfect gate operations – such operations will generally lead to heat dissipation into the environment. Our theoretical model for describing these operations is detailed in the Model section (Sec. IV) of this report.

The overall heat generated from a quantum computer can be broken down into three components: those involving qubit initialization, imperfect gate operations, and qubit measurement. We seek to investigate each of the three on a theoretical level, and incorporate experimental data from near-term quantum computers. We now briefly describe these objectives in the following subsections.

A. Initialization and measurement

In order to attain a full accounting of the heat produced in a quantum algorithm, the costs associated with initialization and measurement must be considered. Initialization, as a process by which an unknown quantum state is transformed into a definite state, is irreversible, and is comparable to a classical erasure protocol. So, just as classical erasure processes are associated with heat dissipation bounded by the Landauer limit, quantum initialization is subject to analogous constraints [9]. Measurement, as another irreversible quantum operation, may have similar thermodynamic costs [10].

B. Building a circuit with gates

Assuming a circuit with n qubits, a maximum gate depth of d, and the associated fidelities of individual gates of depth k to be x_k, we aim to establish an upper bound on the total heat generated by the given circuit as some function $Q(n, d, \{x_k\}_{k=1}^{d})$. We plan to use the quantum channel approach to model the interaction with the bath as has been investigated for small quantum systems. [11, 12]. In the Model section (Sec. IV) of this report, we explain this approach in more detail, and we consider the specific case of single-qubit gates in the presence of a dephasing environment.

Since all quantum algorithms can be represented as quantum circuits [3], we will consider our bounds in the context of specific algorithms, for instance, Shor's algorithm, Grover's algorithm and so on, thereby introducing a nominal "heat complexity" for these algorithms. Such analysis will require the computation of heat values for multi-qubit gates and successive unitary operations. Through an extension of our single-qubit model, it may be possible

to derive bounds relating the total heat generated in a quantum circuit to the heat generated by each circuit component considered in isolation.

C. Near-term quantum computers

We plan to incorporate experimental values in our theoretical calculations from currently established quantum computing platforms, and determine a scale in the number of qubits, gate depth and circuit complexity at which this heat cost can detrimentally affect computation. We may also explore if different implementations and architectures [13–16] can offer different heat costs, and how they can be leveraged for scalability. To this end, we have collected data about existing qubit implementations in the following section.

III. DATA ON CURRENT QUANTUM COMPUTING IMPLEMENTATIONS

In this section, we summarize qubit proposals currently under extensive experimental investigation for building quantum computers. T_1 is roughly the timescale on which the state of the qubit decays (say from $|1\rangle \rightarrow |0\rangle$) while T_2 is the timescale during which coherence is lost ($\frac{|0\rangle+|1\rangle}{\sqrt{2}} \rightarrow |0\rangle$). We begin by briefly explaining the qubit proposals.

- **Spin qubits**: Single electrons confined in solid-state structures called quantum dots are used. Under the application of a magnetic field, the electron-spin states form a two-level system to be used as a qubit.
- **Trapped Ions**: Ions are trapped using radio-frequency dynamic electrical potentials and two electronic states within each ion are used as a qubit. Optical transitions and the Coulomb interaction between ions are used to control the qubit state and measure the qubits.
- **Photonic qubits**: Photonic/optical quantum computing covers a vast array of architectures. The most encompassing paradigm is Linear Optical Quantum Computing (LOQC), wherein qubits are encoded in photons and are manipulated with linear optical elements. The predominate encoding schemes are polarization qubits and time-bin qubits. The optical nature of this architecture makes gate times negligible compared to coherence times.
- **Superconducting (SC) qubits**: An electronic circuit consisting of a capacitor and a Josephson junction provides a macroscopic platform for quantum harmonic oscillators. The harmonic potential is then manipulated in various formats to isolate a two level system. These formats include the two broad categories of charge qubits and flux qubits. The most popular architecture, the transmon, is of a charge qubit design with enhanced protection against charge noise.

Qubit Proposal	T_1	T_2	**Single-qubit gate time**	**Single-qubit gate fidelity**	**Two-qubit gate time**	**Two-qubit gate fidelity**
Spin qubits (GaAs) [17]	1 s	0.44 µs	20 ns	0.86	350 ps (SWAP)	N/A
Spin qubits (SiGe) [18, 19]	N/A	20 µs	40 ns	0.99926	200 ns (CNOT)	0.78
Trapped Ions [20]	$\sim\infty$	0.5 s	20 µs	0.997	250 µs	0.965
Polarization qubits [21, 22]	hours	0.1 ms		0.9984		>0.75
SC (transmon) qubits [23–25]	1 µs	1 µs	15 ns	0.988	190 ns (CNOT)	0.92

TABLE I. T_1, T_2, gate times and fidelities of experimental qubit proposals.

IV. MODEL

A. Overview

One goal of this project is to explore the relationship between entropy production, heat generation, and fidelity in quantum computation. To this end, we develop a model of quantum computation in the presence of an uncontrolled environment, in

which environmental interactions reduce the fidelity of ideal quantum logic operations. The basic structure of our model is as follows.

Consider a quantum logic gate acting on a set of N qubits, carried out by applying the unitary operator $\hat{U} = e^{-i\hat{H}t/\hbar}$. In any real experimental setting, the fidelity with which this gate is implemented is limited by two factors. First, it may not be experimentally feasible to engineer the exact Hamiltonian $\hat{H}$ which generates the required unitary evolution. Second, even if this Hamiltonian could be implemented exactly, interactions with the environment will generically entangle the qubits with the environment, perturbing them away from the desired final state. Due to both of these limitations, the implementation of a quantum gate is inevitably subject to deviations away from ideal performance.

In our model, we restrict our attention to losses of fidelity due to the second of these effects: Interaction with the environment. With this focus in mind, we approximate the implementation of a gate as a two-step process. Assuming that the qubits begin in a pure state $\hat{\rho}_0 = |\psi\rangle\langle\psi|$, we first apply the unitary operation $\hat{U}$ to this initial state. The gate time of $\hat{U}$ is assumed to be short compared to interactions with the environment. During this step, the coupling between the qubits and the environment is ignored, and the system evolves to the pure state $\hat{\rho}_1$:

$$\hat{\rho}_0 \rightarrow \hat{\rho}_1 = \hat{U}\hat{\rho}_0\hat{U}^\dagger \tag{1}$$

Interaction with the environment is modelled in the second step. In this step, the state $\hat{\rho}_1$ is evolved via a quantum channel, with an associated set of Kraus operators $\{\hat{A}_i\}$:

$$\hat{\rho}_1 \rightarrow \hat{\rho}_2 = \sum_i \hat{A}_i\hat{\rho}_1\hat{A}_i^\dagger \tag{2}$$

As a result of this second process, the final state of the qubits, $\hat{\rho}_2$, will generically deviate from the desired state $\hat{\rho}_1$, which would have been achieved in the absence of environmental interaction (see Fig. 1).

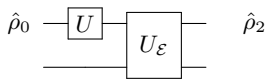

FIG. 1. Effective circuit to model a imperfect unitary operation due to interaction with the environment. As a result, the system state evolves under the action of Kraus operators $\hat{A}_i$ as defined in the text after the action of the unitary $\hat{U}$.

Most of the analysis for this project will be carried out using this two-step evolution framework. We believe that this framework is appropriate since T_2 time (which can be thought as the timescale to interact with the environment) is much larger than individual gate times (see Table I). Note that at this stage, the model is sufficiently general to analyze any N-qubit gate, followed by an arbitrary interaction with the environment. However, we will begin our analysis with a much more specific scenario, detailed in Section IV C, in which the application of a single-qubit gate is followed by a dephasing interaction with the environment.

B. Relevant quantities

To analyze the quantum computation process defined above in (1) and (2), there are several useful quantities that we will consider. We will describe two especially important quantities here: The fidelity loss in a quantum computation, and the entropy change. First, the fidelity F, which characterizes the deviation of a given density operator $\hat{\sigma}$ relative to a "target" operator $\hat{\rho}$, is defined as

$$F \equiv \mathrm{Tr}\left[\sqrt{\sqrt{\hat{\rho}}\hat{\sigma}\sqrt{\hat{\rho}}}\right]. \tag{3}$$

In the context of the two-step evolution protocol defined previously, we would like to compare the true final state of the qubits, represented by $\hat{\rho}_2$, to the target state $\hat{\rho}_1$, which would be obtained if environmental effects could be entirely suppressed. Using the fact that this target states is pure, it is straightforward to show that the fidelity loss ΔF due to the two-step evolution is given by

$$\Delta F = \sqrt{\mathrm{Tr}\left[\hat{\rho}_1\hat{\rho}_2\right]} - 1. \tag{4}$$

For a quantum operation beginning from a pure state, ΔF is necessarily non-positive, and its magnitude quantifies the degree to which the noisy implementation of this operation differs from the ideal case.

Second, we can compute the entropy change associated with a given two-step evolution process. The von Neumann entropy associated with a quantum state $\hat{\rho}$ is defined as $S \equiv -\mathrm{Tr}[\hat{\rho}\ln\hat{\rho}]$. Here and elsewhere, Boltzmann's constant k_B has been set to one. Entropy is one metric for quantifying the impurity of a quantum state: Pure states possess zero entropy, while the maximally mixed state is also the maximum entropy state. Since $\hat{\rho}_0$ and $\hat{\rho}_1$ are both pure states, the entropy change ΔS in the two-step evolution protocol is simply the final entropy, associated with $\hat{\rho}_2$:

$$\Delta S = -\mathrm{Tr}\left[\hat{\rho}_2\ln\hat{\rho}_2\right] \tag{5}$$

In this project, we aim to explore the relationships between these and other quantities of interest, both by establishing analytical bounds and by performing numerical simulations. In addition, we will invoke the quantum Landauer bound [5, 6] to relate the entropy production ΔS to the heat generated during the quantum operation. In some simple models, such as the single-qubit dephasing model described below, we expect that these quantities can be evaluated explicitly in terms of a few relevant parameters.

C. Single-qubit gates with dephasing

In the simplest case, we will perform our analysis in the context of a single qubit, interacting with a dephasing environment. When a qubit undergoes dephasing, the probabilities associated with finding the qubit in either computational basis state $|0\rangle$ or $|1\rangle$ remain fixed, but the coherences between these states are reduced. Such an interaction can be modelled as a quantum channel with two Kraus operators [3]:

$$\hat{A}_1 \equiv \sqrt{\alpha}\hat{I}, \quad \hat{A}_2 \equiv \sqrt{1-\alpha}\hat{Z} \tag{6}$$

Here, $\hat{I}$ is the identity operator, $\hat{Z}$ is the phase flip or Pauli-z operator, and α is a real number between 0 and 1. When this channel is applied to the quantum state $\hat{\rho}_1$, (2) tells us that the resulting state $\hat{\rho}_2$ is given by

$$\hat{\rho}_2 = \alpha\hat{\rho}_1 + (1-\alpha)\hat{Z}\hat{\rho}_1\hat{Z}. \tag{7}$$

Speaking loosely, this evolution may be given the following interpretation: With probability α, the initial state $\hat{\rho}_1$ has been left unchanged; and with probability $1-\alpha$, the phase of the initial state has been flipped.

In this dephasing model, we can compute the fidelity loss (4) and the entropy change (5) as a function of the initial quantum state and the parameter α. We will investigate these two quantities for different ranges of α, and for various choices of initial state. For example, it may be instructive to consider the limit where $\alpha \approx 1$, in which the state remains approximately pure. Ultimately, it may also prove fruitful to generalize this model to multi-qubit gates, with each qubit interacting with an independent dephasing environment.

D. Numerical simulations on the single-qubit dephasing channel

We tried to numerically understand the relationship between ΔS and F for a initial pure state $\hat{\rho}_i$ in the dephasing model. Our simulation proceeded as follows:

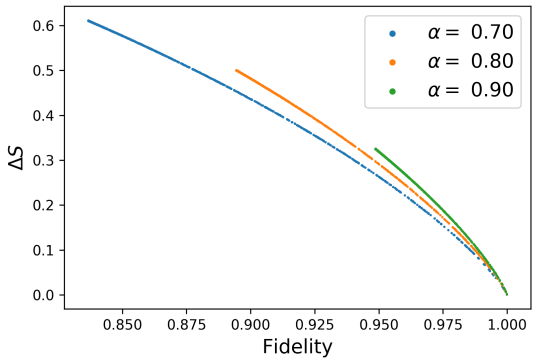

FIG. 2. Effect of the dephasing channel for initial pure states uniformly randomly sampled on the Bloch sphere. We plot the relationship between the change in entropy ΔS and fidelity F between the initial state and after the effect of channel for different values of the channel parameter α.

Simulation algorithm

1. Sample $\hat{\rho}_i$ uniformly on the Bloch sphere. This is equivalent to sampling all possible single qubit gates.
2. Calculate the effect of the dephasing channel on $\hat{\rho}_i$ as $\hat{\rho}_f = \alpha\hat{\rho}_i + (1-\alpha)\hat{Z}\hat{\rho}_i\hat{Z}$
3. Plot the points $(F(\hat{\rho}_f, \hat{\rho}_i), \Delta S = S(\hat{\rho}_f) - S(\hat{\rho}_i))$

Let us first consider some limiting cases. When $F = 1$, then $\hat{\rho}_f = \hat{\rho}_i$ and hence $\Delta S = 0$. This is expected, as when $F = 1$, it is as if the channel has no effect whatsoever, and the entropy change would be zero. Now, for a fidelity not equal to 1, ΔS is finite. Through this simulation we have numerically established that there exists a well-defined relationship between ΔS and F, and that ΔS is small but finite for F close to but less than 1 (see Fig. 2). This finite positive entropy production implies an upper bound on the amount of heat added to the system during the quantum operation, as a consequence of the Second Law of Thermodynamics.

E. Channels on two-qubit gates

Moving on to understanding imperfect two-qubit gates leads to a increased freedom for modelling the environmental interaction. There are no specific models like the dephasing channel that are defined for two-qubit states. We therefore assume a simplistic picture of the environmental interaction, in which each qubit interacts with a separate

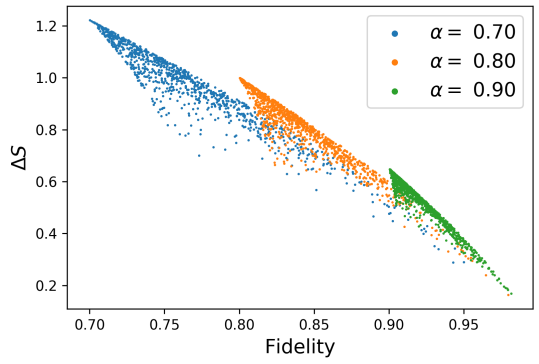

FIG. 3. Effect of the dephasing channel for initial pure states uniformly randomly sampled over two qubits. We plot the relationship between the change in entropy ΔS and fidelity F between the initial state and after the effect of the channel, for different values of the channel parameter α.

bath particular to that qubit. This leads to two qubit Kraus operators $\hat{B}$ defined by taking the tensor product of single qubit Kraus operators:

$$\hat{B}_{ij} = \hat{A}_i \otimes \hat{A}_j, \tag{8}$$

where $\hat{A}_i$ are the Kraus operators for any single qubit channel. We use this model to understand two qubit gate fidelities and entropy change similar to the case of single-qubit gates. The values could then be compared to realistic experimental fidelities (see Sec. III) to understand entropy and hence heat production as a result of environmental interactions. Since two-qubit gate fidelities are generally worse than single-qubit fidelities, we expect this will cause significant scalability issues for near term quantum computers.

Fig. 3 shows the results of our numerical simulations for the entropy generation versus fidelity. This is a scatter plot obtained by starting with a random pure two-qubit state, sampled with respect to the Haar measure. This corresponds to sampling possible two-qubit gates. We they apply the channel with four Kraus operators as defined in the product form (Eqn. 8.) We see many interesting features which we don't fully understand. Instead of a well-defined relationship between ΔS vs F as is seen for the single qubit case (Fig. 2), we instead see a scatter of ΔS values for each F. Also, the scatter is not spread across the possible values of F, which is a restriction caused by our distribution of sampled initial conditions. As only eigenstates of the $\mathrm{Z}^{\otimes N}$ gate result in fidelity 1, the more qubits we add, the more a randomly uniform sampling of initial conditions skews away from the finite amount of said eigenstates.

F. Channels on k-qubit gates

We now move on to numerically understanding the effect of the dephasing channel on the k-qubit case. Just like the two-qubit case, we make the simplifying assumption that each qubit is acted upon by an individual dephasing channel, so the set of all possible Kraus operators is now defined as:

$$\hat{B} = \bigotimes_{l=1}^{k} \hat{A}_l \tag{9}$$

where $\hat{B}$ is the k-qubit Kraus operator and $\hat{A}_l$ are individual qubit Kraus operators.

Fig. 4 shows the scatter plots of the change in entropy ΔS vs fidelity F for $k = 3, 4, 5, 6$ qubits respectively and for three values of the channel parameter $\alpha = 0.7, 0.8, 0.9$. Features present in the two-qubit case reproduced, for instance the scatter of ΔS values for each value of F. The general trend is ΔS values increase for a fixed F approxmiately linearly. The separation between then scatter of values for different α also increases with increasing number of qubits. We believe that the sampling problem becomes severe for larger number of qubits as the parameter space of all pure states increases exponentially. As a result, only a smaller section of the ΔS vs F curve is seen for increasing number of qubits.

V. BOUNDS AND GENERAL DISCUSSION

A. Quantum Landauer bound

In the context of classical computation, the Landauer bound places a lower bound on the amount of heat expelled to the environment during an irreversible logical operation [1]. This bound follows directly from the application of the second law of thermodynamics to a register of classical bits coupled to a thermal bath. For example, for the resetting of a single bit to the zero state, the Landauer bound imposes the following constraint on the amount of heat Q_{ext} released to the bath:

$$Q_{ext} \geq T \ln 2. \tag{10}$$

Here, T is the temperature of the bath.

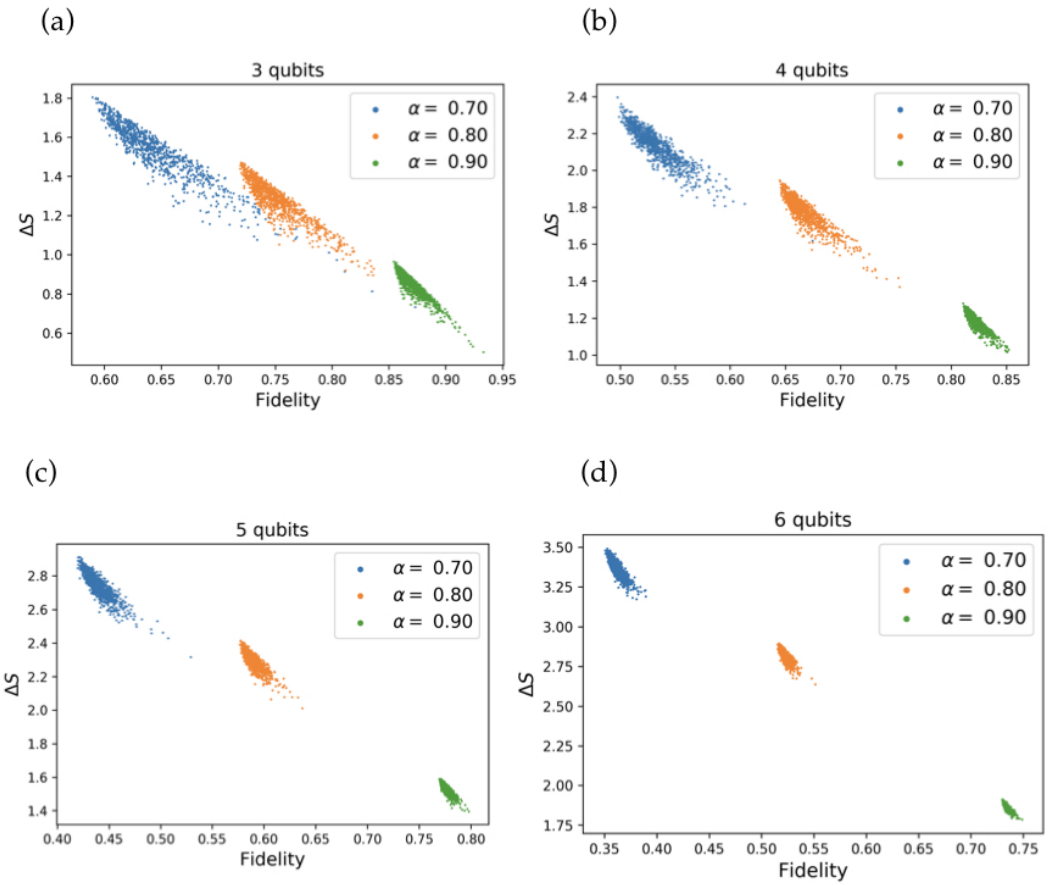

FIG. 4. Effect of the dephasing channel for initial pure states uniformly randomly sampled over 3,4,5 and 6 qubits. We plot the relationship between the change in entropy ΔS and fidelity F between the initial state and after the effect of the channel, for different values of the channel parameter α.

For quantum systems, a version of the second law of thermodynamics can also be derived [4] and therefore statements akin to the classical Landauer bound can be made. For example, in one formulation of quantum thermodynamics [4], the second law may be stated in terms of a type of average heat $\langle Q \rangle$ added to the quantum system of interest, and the von Neumann entropy change ΔS:

$$\Delta S \geq \frac{\langle Q \rangle}{T} \tag{11}$$

For a system with density operator $\hat{\rho}$, the entropy is defined as $S =\equiv -\mathrm{Tr}[\hat{\rho} \ln \hat{\rho}]$, and the definition of $\langle Q \rangle$ takes the form

$$\langle Q \rangle \equiv \int_{t_1}^{t_2} dt \ \mathrm{Tr}\left[\frac{d\hat{\rho}}{dt}\hat{H}\right] \tag{12}$$

for a process between two times t_1 and t_2. $\hat{H}$ denotes the Hamiltonian of the quantum system.

This quantum version of the second law is relevant to our project because it places a bound on the amount of heat absorbed by a quantum system. This may prove to be important for understanding the conditions under which quantum computers experience significant detrimental heating. Specifically, in the following sections we derive that, under a suitable set of assumptions, the combination of the quantum second law and a result called the Fannes inequality yields a relation between the heat absorbed by a quantum system and the fidelity associated with a given quantum operation.

B. Fannes inequality

As the heat generated by a quantum system is bounded by the change in von Neumann entropy, we would like to relate the entropy difference between two quantum state with the trace distance between

the two states of interest. In Fannes' original paper on spin lattices [26], the continuity of the von Neumann entropy is shown to provide the inequality

$$|S(\rho) - S(\sigma)| \leq 2\mathcal{T} \log_2(d) - 2\mathcal{T} \log_2(2\mathcal{T}), \quad (13)$$

where $\mathcal{T}$ is the trace distance given by

$$\mathcal{T}(\rho, \sigma) = ||\rho - \sigma||_1 = \mathrm{Tr}\left[\sqrt{(\rho - \sigma)^\dagger (\rho - \sigma)}\right] \quad (14)$$

and d is just the the dimension of system. This inequality can be further refined for qubit systems to show [27]

$$|S(\rho) - S(\sigma)| \leq \mathcal{T} \log_2(d-1) + H(\mathcal{T}, 1-\mathcal{T}), \quad (15)$$

where H is the (classical) Shannon entropy

$$H(\{p_i\}) = -\sum_i p_i \log p_i. \quad (16)$$

If one were to assume minimal fidelity loss during gate operation, such that the final state σ is perturbatively close to the targeted final state ρ, the trace distance between the two states is small. We note that from the Fuchs-van de Graff inequality [3], for small trace distances

$$\mathcal{T} \approx \epsilon \approx 1 - F. \quad (17)$$

Therefore, we have

$$\begin{aligned} &|S(\rho) - S(\sigma)| && (18)\\ &\leq \mathcal{T} \log_2(d-1) + H(T, 1-T) && (19)\\ &= \epsilon \log_2(d-1) - \epsilon \log \epsilon - (1-\epsilon)\log(1-\epsilon) && (20)\\ &= \epsilon \log_2(d-1) - \epsilon \log \epsilon + \epsilon + O(\epsilon^2). && (21) \end{aligned}$$

For an n-qubit system, $d = 2^n$, giving us

$$|S(\rho) - S(\sigma)| \lessapprox n\epsilon - \epsilon \log \epsilon + \epsilon + O(\epsilon^2), \quad (22)$$

or

$$|\Delta S| \lessapprox n\epsilon. \quad (23)$$

This provides us with an upper bound on entropy change, which can then be used to calculate the heat output of our quantum computer.

C. Upper bound on heat absorption

Using the results of the previous two sections, we may now derive a relation between the heat absorbed by a quantum system during an operation, and the fidelity loss associated with that operation. This result is obtain by simply combining the second law with the bound $n\epsilon \geq |\Delta S| \geq \Delta S$. Chaining this inequality with the second law and multiplying by T yields

$$\langle Q \rangle \leq Tn\epsilon. \quad (24)$$

That is, we find that the heat absorbed by a quantum system during an operation is bounded from above, given the assumptions stated in the previous section. This bound tells us that by keeping the temperature of the environment very low, or by ensuring that the fidelity loss ϵ is minimized, one may be able to place strong limits on how much heat a quantum system absorbs. However, even under such conditions, a large number of qubits n means that this bound will be very high.

D. Architecturally dependent bounds

Using a rough physical argument, we can make some final general claims about the scaling of heat absorption in quantum computers. Specifically, we argue that the growth of heat absorption as a function of number of qubits will depend on whether the physical architecture of the computer is one, two, or three-dimensional.

Suppose that, over a given amount of time, a typical qubit which is interacting with its environment absorbs an amount of heat q. Given this typical heat flow per qubit, let us examine how the dimensionality of the quantum computer is related to the *total* heat absorbed by the whole computer. First, consider the case where the computer consists of a one-dimensional array of n qubits. If we assume that appreciable heat flow only occurs at the ends of the array, then the total amount of heat absorbed will be of order q, and approximately independent of n.

The situation changes if we move to two dimensions. For a two-dimensional grid of n qubits, which can exchange heat with the environment only along the edges, the total heat absorbed will be on the scale of $n^{1/2}q$. This is because the number of qubits interacting with the environment is proportional to the total edge length, which scales proportional to $n^{1/2}$. Finally, by an analogous argument, the total heat absorbed by a three-dimensional quantum computer will be of order $n^{2/3}q$, assuming that heat can only flow into the computer via its surface.

The consequence of the dimensionality of the architectures is that they will have different bounds on the maximum number of qubits. The heat generated, as found in the previous section, scales as

$$Q \lessapprox T\Delta S \approx \epsilon n T. \quad (25)$$

Therefore, for example, a 2D system able to dissipate $\sqrt{n}T$ of heat will have an upper bound on n of

$$Q \lessapprox \epsilon n T < \sqrt{n} T \tag{26}$$

$$\Rightarrow n \lessapprox \frac{1}{\epsilon^2}, \tag{27}$$

whereas a 3D system is bound by

$$Q \lessapprox \epsilon n T < n^{2/3} T \tag{28}$$

$$\Rightarrow n \lessapprox \frac{1}{\epsilon^3}, \tag{29}$$

VI. OPEN PROBLEMS AND FUTURE WORK

In this project, our aim has been to make connections between fidelity, entropy generation, and heat flow in quantum circuits. Exploring these relationships naturally leads to several other potential topics of investigation. Chiefly among these is the relaence of the quantum Landauer bound: as the heat generated by modern classical computations is orders of magnitude above the Landauer bound [2], this bound imposes no practical restrictions on circuit design. In contrast to this, will the *quantum* Landauer bound prove to be practically relevant in the design of quantum circuits?

In addition, there are also some general conceptual issues in the fields of quantum computation and quantum thermodynamics which our work is adjacent to. These include:

- *Definitions of thermodynamic quantities in the quantum realm:* Many distinct definitions of heat and work have been proposed for quantum systems [28]. Which ones are most useful for understanding quantum computation?
- *Thermodynamics of measurement:* How can quantum measurement be treated as a thermodynamic process, and how will the thermodynamic costs of measurement affect the functioning of quantum circuits?
- *Comparisons of quantum and classical computations:* The superiority of quantum computation is usually expressed in terms of computational complexity. Do certain quantum algorithms also possess a "thermodynamic advantage" over their classical counterparts?

In conclusion, we have established a quantum channel model for dealing with imperfect unitary operations. We evaluated our model with the dephasing channel for a single and multi qubit system, establishing a framework to help understand imperfect unitaries. At the end, we investigated limitations on scalability due to heat arising from imperfect gates for near-term quantum computers.

[1] R. Landauer, IBM Journal of Research and Development .

[2] "Tikalon blog by dev gualtieri," http://tikalon.com/blog/blog.php?ARTICLE=2011/Landauer, (Accessed on 09/20/2018).

[3] M. A. Nielsen and I. L. Chuang, *Quantum Computation and Quantum Information: 10th Anniversary Edition*, 10th ed. (Cambridge University Press, New York, NY, USA, 2011).

[4] S. Vinjanampathy and J. Anders, arXiv:1508.06099v2 arXiv:arXiv:1508.06099v2.

[5] D. Reeb and M. M. Wolf, New Journal of Physics **16**, 103011 (2014).

[6] J. Goold, M. Huber, A. Riera, L. Del Rio, and P. Skrzypczyk, Journal of Physics A: Mathematical and Theoretical **49** (2016), 10.1088/1751-8113/49/14/143001, arXiv:1505.07835.

[7] T. D. Ladd, F. Jelezko, R. Laflamme, Y. Nakamura, C. Monroe, and J. L. O'Brien, Nature **464**, 45 (2010).

[8] D. P. DiVincenzo, Fortschritte der Physik **48**, 771 (2000).

[9] D. J. Bedingham and O. J. E. Maroney, New Journal of Physics **18**, 113050 (2016).

[10] M. H. Partovi, Physics Letters A **137**, 445 (1989).

[11] J. Goold, M. Paternostro, and K. Modi, Phys. Rev. Lett. **114**, 060602 (2015).

[12] J. P. S. Peterson, R. S. Sarthour, A. M. Souza, I. S. Oliveira, J. Goold, K. Modi, D. O. Soares-Pinto, and L. C. Céleri, **472** (2016), 10.1098/rspa.2015.0813.

[13] "IBM Q - Quantum Computing," https://www.research.ibm.com/ibm-q/.

[14] "Home — Rigetti," https://www.rigetti.com/.

[15] "Trapped Ion Quantum Information," http://iontrap.umd.edu/.

[16] L. R. Schreiber and H. Bluhm, **359**, 393 (2018).

[17] C. Kloeffel and D. Loss, Annual Review of Condensed Matter Physics **4**, 51 (2013).

[18] J. Yoneda, K. Takeda, T. Otsuka, T. Nakajima, M. R. Delbecq, G. Allison, T. Honda, T. Kodera, S. Oda, Y. Hoshi, N. Usami, K. M. Itoh, and S. Tarucha, Nature Nanotechnology **13**, 102 (2018).

[19] D. M. Zajac, A. J. Sigillito, M. Russ, F. Borjans, J. M. Taylor, G. Burkard, and J. R. Petta, Science **359**, 439 (2018).

[20] N. M. Linke, D. Maslov, M. Roetteler, S. Debnath, C. Figgatt, K. A. Landsman, K. Wright, and C. Monroe, Proceedings of the National Academy of Sciences **114**, 3305 (2017).

[21] J. C. F. Matthews, A. Politi, A. Stefanov, and J. L. O'Brien, Nature Photonics **3**, 346 (2009).

[22] J. L. O'Brien, G. J. Pryde, A. G. White, T. C. Ralph, and D. Branning, Nature **426**, 264 (2003).

[23] J. A. Schreier, A. A. Houck, J. Koch, D. I. Schuster, B. R. Johnson, J. M. Chow, J. M. Gambetta, J. Majer, L. Frunzio, M. H. Devoret, S. M. Girvin, and R. J. Schoelkopf, Phys. Rev. B **77**, 180502 (2008).

[24] T. W. Larsen, K. D. Petersson, F. Kuemmeth, T. S. Jespersen, P. Krogstrup, J. Nygård, and C. M. Marcus, Phys. Rev. Lett. **115**, 127001 (2015).

[25] S. Rosenblum, Y. Y. Gao, P. Reinhold, C. Wang, C. J. Axline, L. Frunzio, S. M. Girvin, L. Jiang, M. Mirrahimi, M. H. Devoret, and R. J. Schoelkopf, Nature Communications **9**, 652 (2018).

[26] M. Fannes, Commun.Math. Phys. **31**, 291 (1973).

[27] K. M. R. Audenaert, J. Phys. A: Math. Theor. **40**, 8127 (2007).

[28] P. Talkner and P. Hänggi, Phys. Rev. E **93**, 022131 (2016).